

Related topics

Bohr's atomic model, quantisation of energy levels, electron spin, Bohr's magneton, interference of electromagnetic waves, Fabry-Perot interferometer.

Principle and task

The "Zeeman effect" is the splitting up of the central spectral lines of atoms within a magnetic field. The simplest is the splitting up of one spectral line into three components called the "normal Zeeman effect". The normal Zeeman effect is studied using a cadmium spectral lamp as a specimen. The cadmium lamp is submitted to different magnetic flux densities and the splitting up of the red cadmium line (643.8 nm) is investigated using a Fabry-Perot interferometer. The evaluation of the results leads to a fairly precise value for Bohr's magneton.

Equipment

Fabry-Perot interferometer	09050.02	1
Cadmium lamp f. Zeeman effect	09050.01	1
Electromagnet w/o pole shoes	06480.01	1
Pole piece, drilled, conical	06480.03	1
Rot.table for heavy loads	02077.00	1
Power supply for spectral lamps	13662.93	1
Var.transformer, 25 VAC/20 VDC, 12 A	13531.93	1
Capacitor, electrolyt., 22000 mic-F	06211.00	1
Digital multimeter	07134.00	1
Optical profile-bench, l 1000 mm	08282.00	1
Base f. opt. profile-bench, adjust.	08284.00	2
Slide mount, lateral.adjust., cal.	08082.03	1
Slide mount f. opt. pr.-bench, h 30 mm	08286.01	5

Slide mount f.opt.pr.-bench, h 80 mm	08286.02	1
Lens holder	08012.00	4
Lens, mounted, f +50 mm	08020.01	2
Lens, mounted, f +300 mm	08023.01	1
Iris diaphragm	08045.00	1
Polarising filter, on stem	08610.00	1
Polarization specimen, mica	08664.00	1
Screen, with aperture and scale	08340.00	1
Plate holder with tension spring	08288.00	1
Swinging arm	08256.00	1
Spirit level	02124.00	1
Connecting cord, 500 mm, red	07361.01	2
Connecting cord, 500 mm, blue	07361.04	2

Problems

1. Using the Fabry-Perot interferometer and a selfmade telescope the splitting up of the central line into two σ -lines is measured in wave numbers as a function of the magnetic flux density.
2. From the results of point 1. a value for Bohr's magneton is evaluated.
3. The light emitted within the direction of the magnetic field is qualitatively investigated.

Set-up and procedure

The electromagnet is put on the rotating table for heavy loads and mounted with the two pole-shoes with holes in such a way that a gap of 9 mm remains for the Cd-lamp. The pole-shoes have to be well tightened in such a way that they can-

Fig.1: Experimental set-up for the Zeeman effect.



not move later on when the magnetic flux is established. The Cd-lamp is inserted into the gap without touching the pole-shoes and connected to the power supply for spectral lamps. The coils of the electromagnet are connected in parallel and via an ammeter connected to the variable power supply of up to 20 VDC, 12 A. A capacitor of 22 000 μF is in parallel to the power output to smoothen the DC-voltage.

The optical bench for investigation of the line splitting carries the following elements (their approximate position in cm is given in brackets):

- (63) $L_3 = +50$ mm
 - (57.5) Screen with scale
 - (38.5) Analyser
 - (24.5) $L_2 = +300$ mm
 - (16.5) Fabry-Perot Etalon
 - (9) $L_1 = +50$ mm
 - (4) Iris diaphragm
 - (0) Drilled pole-shoes
- CD-spectral lamp
Rotating table

The iris diaphragm is eliminated for initial adjustment and for the observation of the longitudinal Zeeman effect. During observation of the transverse Zeeman effect the iris diaphragm is illuminated by the Cd-lamp and acts as such as the light source. The lens L_1 and a lens of $f = 100$ mm, incorporated in the étalon, create a nearly parallel light beam which the Fabry-Perot étalon needs for a proper interference pattern. The étalon contains an interchangeable colour filter which filters out the red cadmium line of 643.8 nm. The lens L_2 produces an interference pattern of rings within the plane of the screen with a scale mounted on a slide mount which can laterally be displaced with a precision of 1/100 of a millimeter. The ring system is observed through L_3 and the ring diameters can be measured, for instance, by systematic displacement of the slash representing the "0" of the scale. The readings should be done in a completely darkened room using a flashlight.

The initial adjustment is done in the following way:

The rotating table with electromagnet, pole-shoes and Cd-lamp already mounted is brought to a height of about 16 cm above table using the supporting blocks. By means of the spirit level, the electromagnet is adjusted perfectly horizontal. The optical bench with all elements (except is iris diaphragm) mounted, is then moved closer to the electromagnet in such a way that one of the outlet holes of the pole-shoes coincides with the previous position of the iris diaphragm. L_1 is then adjusted so that the outlet hole is within the focus of it. All other optical elements of Fig. 2. are subsequently readjusted with respect to their height correspondingly. The current of the coils is set for some time to 8 [A] (increase in light intensity!) and the ring interference pattern in axial direction is observed through L_3 . The pattern must be centered and sharp which is eventually achieved by a last, slight movement of the étalon (to the right or to the left) and by displacement of L_2 (vertically and horizontally). Finally the screen with scale is shifted in a way that the slash representing the "0" of the scale is clearly seen coinciding, for instance, with the center of the fairly bright inner ring. The scale itself must be able to move horizontally along the diameter of the ring pattern.

The electromagnet is now turned by 90° , the iris diaphragm is inserted and the analyser turned until the π -line (expl. follows) disappears completely and the two σ -lines appear clearly visible.

Remark: For later evaluations the calibration curve of the magnetic flux density versus the coil current has to be traced previously. This can be done if a teslameter is available. Otherwise the results of Fig. 3 must be used. The curve of Fig. 3 was traced by measuring the flux density in the center of the gap in the absence of the Cd-lamp. For the evaluations these center-values were increased by 3.5% to account for the non-uniform flux distribution within the gap.

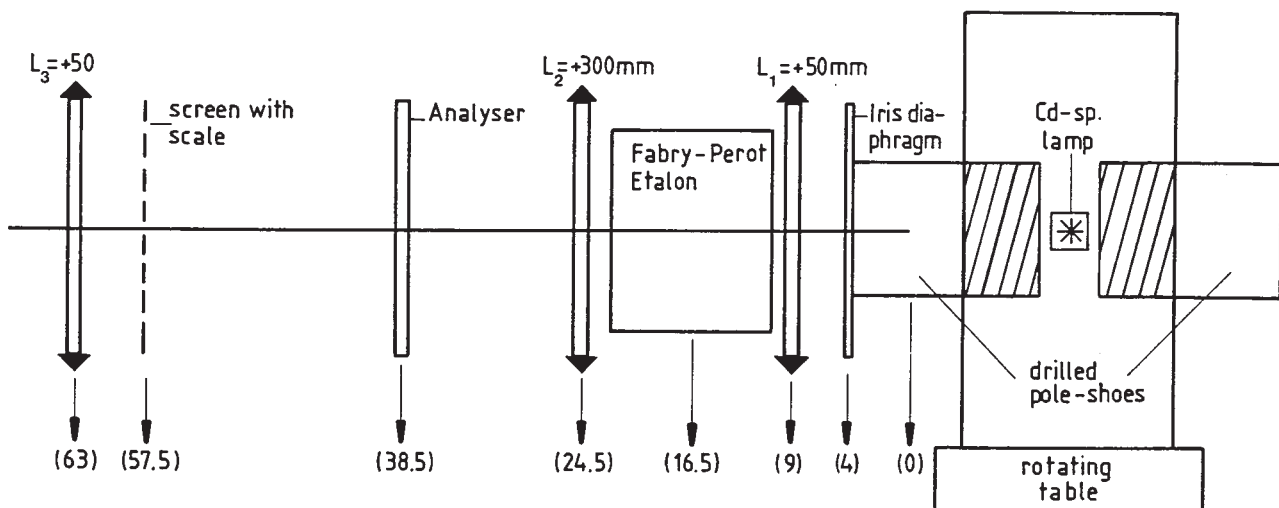
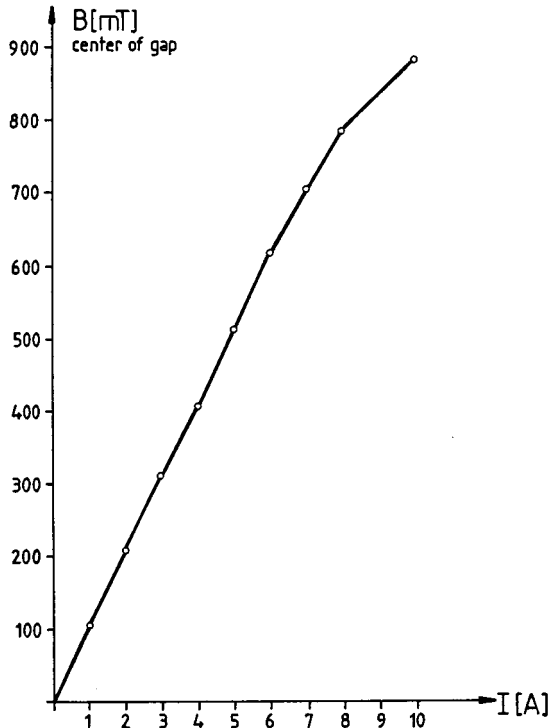


Fig. 2: Arrangement of the optical components.

Fig. 3: Magnetic flux density B in the center of gap without the Cd-lamp (gab width: 9 mm) as a function of the coil current.



Theory and evaluation

As early as 1862, Faraday investigated whether the spectrum of coloured flames changes because of the effect of a magnetic field, but without success. It was not until 1885 that the Belgian Fizeau was able to demonstrate an effect, but it was forgotten and only rediscovered 11 years later by the Dutchman Zeeman, who studied it together with Lorentz.

This experiment, which was of importance to the development of the theory of the atomic shell, can now be carried out with modern equipment in the students' experiment laboratory.

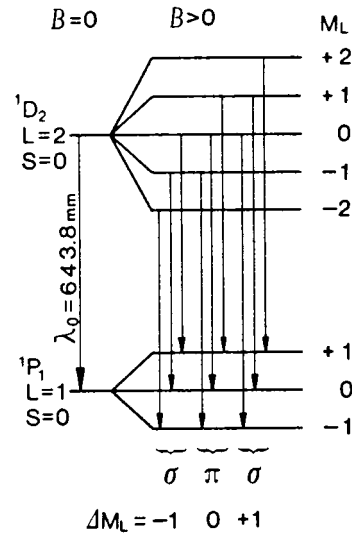
The splitting of the Cd-spectral line $\lambda = 643.8$ nm into three lines, the so-called Lorentz triplets, occurs since the Cd-atom represents a singlet system of total spin $S = 0$. In the absence of a magnetic field there is only one possible $D \rightarrow P$ transition of 643.8 nm, as indicated by Fig. 4.

In the presence of a magnetic field the associated energy levels split into $2L + 1$ components. Radiating transitions between these components are possible, provided that the selection rules

$$\Delta M_L = +1; \Delta M_L = 0; \Delta M_L = -1$$

are taken into account. In this case, therefore, there are a total of nine permitted transitions, only three of which ever have the same energy and hence the same wavelength. Therefore, only three lines will be visible.

Fig. 4: Splitting up of the components in the magnetic field and permitted transitions.



The first group where $\Delta M_L = -1$ gives a σ -line whose light is polarized vertically to the magnetic field. The middle group $\Delta M_L = 0$ gives a π -line whose light is polarized parallel to the direction of the field. The last group where $\Delta M_L = +1$ gives a σ -line whose light is again polarized vertically to the magnetic field.

In the absence of the analyser all three lines can be seen simultaneously. Each ring which was observed in the absence of a magnetic field is split into three rings when a magnetic field is applied. Inserting the analyser the two σ -lines can be observed exclusively if the analyser is in the vertical position, while only the π -line appears if the analyser is turned into its horizontal position (transverse Zeeman effect). Turning the electromagnet by 90° the light coming from the spectral lamp parallel to the direction of the field can also be studied since the pole-shoes have been drilled. It can be shown that this light is circularly polarized light. Whatever the position of the analyser may be, each of the rings seen without a magnetic field is now permanently split into two rings in the presence of a magnetic field (longitudinal Zeeman effect). Fig. 5 summarizes the facts.

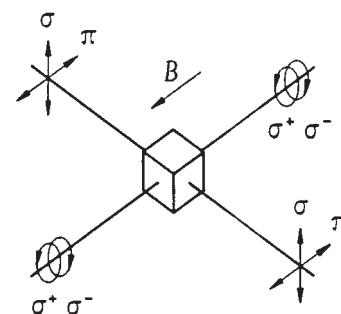
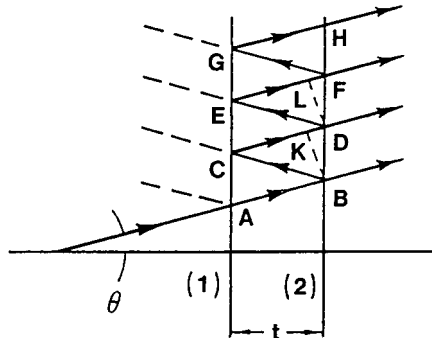


Fig. 5: Longitudinal and transverse Zeeman effect.

Fig. 6: Reflected and transmitted rays at the parallel surfaces (1) and (2) of the étalon. The étalon spacing is t .



Turning the electromagnet back for the observation of the two σ -lines of the transverse Zeeman effect it is easy to see that the size of the splitting increases with increasing magnetic field strength. For a quantitative measurement of this splitting in terms of number of wavelengths, a Farby-Perot interferometer is used, the functioning of which may briefly be explained.

The Fabry-Perot étalon has a resolution of approximately 300000. That means that a wavelength change of approximately 0.002 nm can still be detected.

The étalon consists of two parallel flat glass plates coated on the inner surface with a partially transmitting metallic layer. Let us consider the two partially transmitting surfaces (1) and (2) in Fig. 6 separated by a distance t . An incoming ray making an angle Θ with the normal to the plates will be split into the rays AB, CD, EF, etc. the path difference between the wave fronts of two adjacent rays (for example, AB and CD) is

$$\delta = BC + CK$$

where, obviously, BK is normal to CD. With

$$CK = BC \cos 2 \Theta \text{ and } BC \cos \Theta = t$$

we obtain

$$\begin{aligned} \delta &= BCK = BC (1 + \cos 2\Theta) \\ &= 2 BC \cos^2 \Theta \\ &= 2 t \cos \Theta \end{aligned}$$

and for a constructive interference to occur

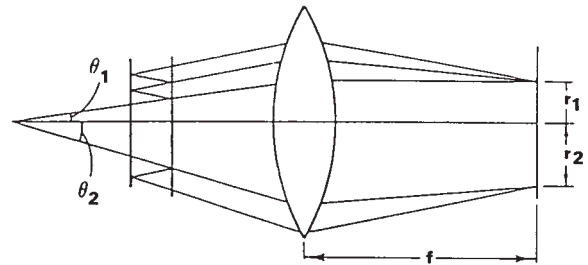
$$n\lambda = 2 t \cos \Theta$$

where n is an integer. If the refractive index of the medium between the plates is $\mu \neq 1$, the equation still has to be modified in the following way:

$$n\lambda = 2 \mu t \cos \Theta \quad (1)$$

Equation (1) is the basic interferometer equation. Let the parallel rays B, D, F, etc. be brought to a focus by the use of a lens of focal length f as shown in Fig. 7.

Fig. 7: Focusing of the light emerging from a Farby-Pero étalon. Light entering the étalon at an angle Θ is focused onto a ring of radius $r = f\Theta$ where f is the focal length of the lens.



Then, when Θ fulfills equation (1), bright rings will appear in the focal plane, their radius being given by

$$r_n = f \tan \Theta_n \approx f \Theta_n \quad (2)$$

for small values Θ_n , e. g. rays nearly parallel to the optical axis.

Since

$$\begin{aligned} n &= \frac{2 \mu t}{\lambda} \cos \Theta_n = n_0 \cos \Theta_0 \\ &= n_0 \left(1 - 2 \sin^2 \frac{\Theta_n}{2} \right) \end{aligned}$$

with

$$n_0 = \frac{2 \mu t}{\lambda}$$

we finally obtain

$$n = n_0 \left(1 - \frac{\Theta_n^2}{2} \right)$$

$$\text{or } \Theta_n = \sqrt{\frac{2(n_0 - n)}{n_0}} \quad (3)$$

If Θ_n is to correspond to a bright fringe, n must be an integer. However, n_0 , which gives the interference at the center ($\cos \Theta = 1$ or $\Theta = 0$ in equation [1]), is in general not an integer. If n_1 is the interference order of the first ring, clearly $n_1 < n_0$ since $n_1 = n_0 \cos \Theta_{n_1}$. We then let

$$n_1 = n_0 - \varepsilon ; 0 < \varepsilon < 1$$

where n_1 is the closest integer to n_0 (smaller than N_0). Thus, we have in general for the p -th ring of the pattern, as measured from the center out,

$$n_p = (n_0 - \varepsilon) - (p - 1) \quad (4)$$

Combining equation (4) with equations (2) and (3), we obtain for the radii of the rings, substituting r_p for r_{n_p} ,

$$r_p = \sqrt{\frac{2f^2}{n_0} \cdot \sqrt{(p-1) + \varepsilon}} \quad (5)$$

we note that the difference between the squares of the radii of adjacent rings is a constant:

$$r_{p+1}^2 - r_p^2 = \frac{2f^2}{n_0} \quad (6)$$

ε can be determined graphically plotting r_p^2 versus p and extrapolating to $r_p^2 = 0$.

Now, if there are two components of a spectral line (splitting of one central line into two components) with wavelengths λ_a and λ_b , which are very close to one another, they will have fractional orders at the center ε_a and ε_b :

$$\varepsilon_a = \frac{2\mu t}{\lambda_a} - n_{1,a} = 2\mu t \bar{\nu}_a - n_{1,a}$$

$$\varepsilon_b = \frac{2\mu t}{\lambda_b} - n_{1,b} = 2\mu t \bar{\nu}_b - n_{1,b}$$

where $n_{1,a}$, $n_{1,b}$ is the interference order of the first ring. Hence, if the rings do not overlap by a whole order $n_{1,a} = n_{1,b}$ and the difference in wave numbers between the two components is simply

$$\Delta \bar{\nu} = \bar{\nu}_a - \bar{\nu}_b = \frac{\varepsilon_a - \varepsilon_b}{2\mu t} \quad (7)$$

Furthermore, using equations (5) and (6), we get

$$\frac{r_{p+1,a}^2}{r_{p+1}^2 - r_p^2} - p = \varepsilon \quad (8)$$

Applying equation (8) to the components a and b , yields

$$\frac{r_{p+1,a}^2}{r_{p+1,a}^2 - r_{p,a}^2} - p = \varepsilon_a$$

and

$$\frac{r_{p+1,b}^2}{r_{p+1,b}^2 - r_{p,b}^2} - p = \varepsilon_b$$

By substituting these fractional orders into equation (7), we get for the difference of the wave numbers:

$$\Delta \bar{\nu} = \frac{1}{2\mu t} \left(\frac{r_{p+1,a}^2}{r_{p+1,a}^2 - r_{p,a}^2} - \frac{r_{p+1,b}^2}{r_{p+1,b}^2 - r_{p,b}^2} \right) \quad (9)$$

From equation (6) it is clear that the difference between the squares of the radii of component a ,

$$\Delta_a^{p+1,p} = r_{p+1,a}^2 - r_{p,a}^2 = \frac{2f^2}{n_{0,a}}$$

is equal to (within a very small part) the same difference for component b

$$\Delta_b^{p+1,p} = r_{p+1,b}^2 - r_{p,b}^2 = \frac{2f^2}{n_{0,b}}$$

Hence,

$$\Delta_a^{p+1,p} = \Delta_b^{p+1,p}$$

whatever the value of p may be. Similarly, all values

$$\delta_{a,b}^{p+1,p} = r_{p+1,a}^2 - r_{p+1,b}^2$$

must be equal, regardless of p and their average can be taken as may be done for the different Δ -values. With δ and Δ as average values we get for the difference of the wave numbers of the components a and b , anticipating $\mu = 1$,

$$\Delta \bar{\nu} = \frac{1}{2t} \frac{\delta}{\Delta} \quad (10)$$

Equation (10)* gives evidence of the fact that $\Delta \bar{\nu}$ does not depend on the dimensions used in measuring the radii of the ring system nor on the amplification of the interference pattern.

1. Provided the ring pattern has been properly established as explained above, the slash of the scale "0" is shifted horizontally along a diameter through the ring pattern until it coincides, for instance, with the fourth ring to the left. A magnetic field corresponding to a coil current of 4 A is established and the splitting of the rings observed. The analyser is put into the vertical position so that only the two σ -lines appear. The "0" slash is now adjusted to coincide perfectly with the outer ring of the two rings, into which the fourth ring has split. The first reading on the socket of the sliding mount is taken. The "0" slash is then moved from left to right through all the rings. The last reading is taken when the "0" slash coincides with the outer ring of the fourth ring to the right. The last reading minus the first reading divided by two then provides the radius $r_{4,b}$. Evaluating the previous readings in a similar way leads to the following radii:

$$I = 4 \text{ [A]: } r_{4,b}; r_{4,a}; r_{3,b}; r_{3,a}; r_{2,b}; r_{2,a}; r_{1,b}; r_{1,a}$$

Further sets of radii are received when repeating the procedure, for instance, for coil currents of 5 A, 6 A, 8 A and 10 A. Using the slide mount, all readings are done in "mm" with a precision of 1/100 th of a mm. Still, the dimension used is not significant since it cancels out when evaluating $\Delta \bar{\nu}$ due to equation (10).

For each set of radii the following square array can be formed:

component	ring number			
	1	2	3	4
a	$r_{1,a}^2 \Delta_a^{2,1}$	$r_{2,a}^2 \Delta_a^{3,2}$	$r_{3,a}^2 \Delta_a^{4,3}$	$r_{4,a}^2$
	$\delta_{a,b}^1$	$\delta_{a,b}^2$	$\delta_{a,b}^3$	$\delta_{a,b}^4$
b	$r_{1,b}^2 \Delta_b^{2,1}$	$r_{2,b}^2 \Delta_b^{3,2}$	$r_{3,b}^2 \Delta_b^{4,3}$	$r_{4,b}^2$

The mean values Δ and δ are calculated here in the following way:

$$\Delta = \frac{1}{4} \sum_{p=1}^2 (\Delta_a^{2p,2p-1} + \Delta_b^{2p,2p-1})^{**}$$

$$\delta = \frac{1}{4} \sum_{p=1}^4 \delta_{a,b}^p$$

The étalon spacing is $t = 3 \cdot 10^{-3}$ [m].

* Milissinow, Adv. Exp. in modern Physics

** Note that not every available Δ -value can be used. Only alternate ones avoid loss of information.

Equation (10) was used to calculate the difference in wave numbers of the two σ -lines as a function of the magnetic flux density and the coil current respectively. The following table summarizes the results:

I [A]	B [mT]	$\Delta\bar{\nu}$ [m^{-1}]
4	417	43.0
5	527	52.2
6	638	59.0
8	810	75.4
10	911	83.6

2. The difference in wave numbers of one of the σ -lines with respect to the central lines is $\Delta\bar{\nu}/2$. For the radiating electrons this means, for instance, a change in energy of

$$\begin{aligned} \Delta E &= E_{L,M_L} - E_{L-1,M_L-1} \\ &= hc \frac{\Delta\bar{\nu}}{2} \end{aligned} \quad (11)$$

On the other hand the change in energy ΔE is proportional to the magnetic flux density B . The factor of proportionality between ΔE and B is μ_B , Bohr's magneton.

$$\Delta E = \mu_B B \quad (12)$$

Combining equations (11) and (12) results in an expression for μ_B :

$$\mu_B = hc \frac{\Delta\bar{\nu}}{2} \frac{1}{B} \quad (13)$$

In Fig. 8 $\Delta\bar{\nu}/2$ was plotted versus the magnetic flux density B . From the regression-line we find a mean value for

$$\frac{\Delta\bar{\nu}}{2} \frac{1}{B}$$

and its standard deviation. Hence,

$$\begin{aligned} \mu_B &= hc \left(\frac{\Delta\bar{\nu}}{2} \frac{1}{B} \right) \\ &= (9.06 \pm 0.46) 10^{-24} \frac{\text{J}}{\text{T}} \end{aligned}$$

The literature value for Bohr's magneton is:

$$\mu_{B,\text{Lit.}} = (9.273) 10^{-24} \frac{\text{J}}{\text{T}}$$

3. The electromagnet is turned by 90° to observe the longitudinal Zeeman effect. In the presence of a magnetic field (a coil current of 8 A is recommended) each of the rings is always split up into two, whatever the position of the analyser may be.

A $\lambda/4$ -plate is generally used to convert linear into elliptical polarized light. In this experiment the $\lambda/4$ -plate is used in the opposite way. Namely, by means of the $\lambda/4$ -plate, inserted manually between L_2 and the analyser, the light of the longitudinal Zeeman effect is investigated. If the optic axis of the $\lambda/4$ -plate coincides with the vertical, it is observed that one ring disappears if the analyser includes an angle of $+45^\circ$ with the vertical while the other ring disappears for a position of -45° . That means that the light of the longitudinal Zeeman effect is polarized in a circular (opposed way).

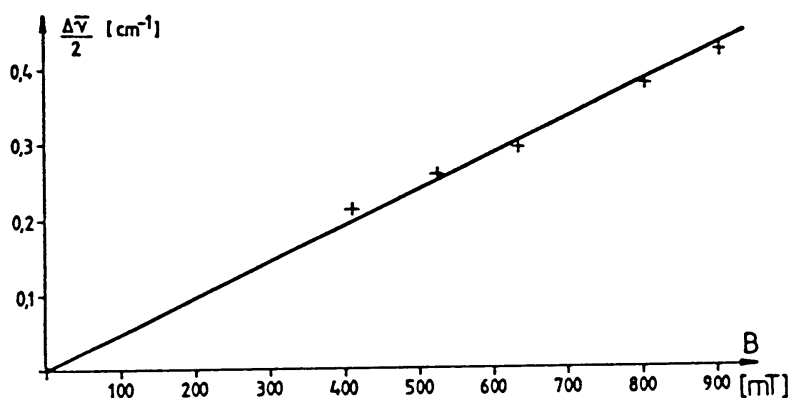


Fig. 8: Zeeman splitting of spectral line $\lambda = 643.8$ nm as a function of Flux density B .